

Computational Analysis of Bell Nozzles

Beena D. Baloni, Sonu P. Kumar, S. A. Channiwala

Department of Mechanical Engineering SVNIT, Surat
Gujarat-395007, India

pbr@med.svnit.ac.in; sonupkumar007@gmail.com; sac@med.svnit.ac.in

Abstract - A Bell type nozzle is most commonly used shape for rocket nozzles. This type of nozzle not only offers significant advantages in terms of size and performance over the conical nozzle but also reduces complexity compared to annular nozzles. The nozzle uses the stagnation temperature (T_0) and stagnation pressure (P_0) generated in the combustion chamber to create thrust by accelerating the combustion gases to a high supersonic velocity. The nozzle expansion ratio was governed by the exit velocity. During flight, the jet flow is ideally expanded and adapted to the surrounding flow only during a short period. The rest of the time, the rocket engine operates in off-design conditions. The present work incorporates 2D axisymmetric flow analysis within the bell type nozzle, at design and off-design conditions, by using computational fluid dynamic software GAMBIT 2.4.6 and FLUENT 6.3.26. A computer code, with the use of the method of characteristics and stream function, is developed to define the higher efficiency nozzle contours for analysis. Simulation has been carried out separately for two different flow conditions i.e. cold and hot. Shear Stress Transport k- ω turbulence model has been chosen for flow analysis. The converged solutions captured asymmetric lambda shock in the nozzles at higher nozzle pressure ratios (NPR) for viscous flows. It also predicted aftershock and flow separation depending upon NPR. The strength of the normal shock, at Mach stem in viscous prediction, generally increases with an increase in NPR. Good agreement is observed between predicted simulation and analytical results in terms of shock structure, shock location, the size of normal shock, aftershock, and asymmetric lambda shocks.

Keywords: Bell type Nozzle, Numerical Analysis, Compressive Waves (Shock Wave)

1. Introduction

A rocket nozzle is a propelling nozzle (usually of the de Laval type) used in a rocket engine to expand and accelerate the combustion gases produced by burning propellants. The hot pressurized gas, passing through the nozzle, is converted to a supersonic speed due to the conversion of heat energy into kinetic energy. Because of this, it is an essential part of the modern rocket engine. To accelerate the air, a favorable pressure gradient must be exerted across the nozzle. At design conditions, the back pressure is similar to nozzle exit pressure and flow accelerates throughout the nozzle. But, at off design conditions, the pressure distribution as well as flow conditions at the exit of the nozzle are varying with variation of back pressure. Flow may be in subsonic, choked, under-expanded or over-expanded conditions at the exit of the supersonic nozzle. One can observe a shock phenomenon in the divergent part and at the exit of the nozzle for back pressures lower than the back pressure needed for choked flow condition. The nozzle is over-expanded ($P_e < P_a$) at lower altitudes than design altitude and under-expanded ($P_e > P_a$) at higher altitudes than design altitude. When the rocket engine operates in off-design conditions, compression and expansion waves are formed around the exhaust jet, with consequent density discontinuities, which gradually achieve a match between the pressure in the jet and the ambient pressure.

Any off-design operation with either over-expanded or under-expanded of exhaust flow induces performance losses. These inherent losses due to non-adapted flow condition for fixed geometry nozzles may rise up to 15%, compared to a continuously adapted exhaust flow [1]. The expansion in the supersonic bell nozzle was more efficient than in a simple straight cone of similar area ratio and length, as the wall contour of bell type was designed to minimize losses [2]. The initial expansion occurs along contour immediately after the throat region in the nozzle. This determines the character of the downstream flow field. Choosing a corner expansion as the initial expansion region yields a slightly shorter nozzle than the one obtained with a radius downstream of the throat for any given expansion ratio. However, in rocket application a sharp corner downstream the throat was generally avoided due to chemical kinetics effects and a wall contour. A nozzle having a radius of curvature equal to 0.5 times the throat radius, were widely used [3]. In parabolic nozzles, side loads occurred as a result of flow transition from free shock separation (FSS) where the flow detaches from the wall after

separation to restricted shock separation(RSS) where the flow re-attaches to the wall after separation and vice versa. The cap-shock pattern was identified to be the cause of this transition [4-8]. At low NPR, internal shock interacts with separation induced shock and then, as NPR increases, it interacts with the Mach disk. If the internal shock was strong, its interaction with the Mach disk caused the annular jet of supersonic flow to deflect outward and reattach to the nozzle wall [9, 10]. Because of the boundary layer, the normal shock ends by lambda-shock structures [11]. If separation at the nozzle wall is asymmetric, large eddies formed in the shear layer of the large separation region, sometimes occupying over half the test section height [12]. These eddies were due to the unsteady nature of the main shock and the instability mechanism was due to an interaction between the expansion fan reflected from the smaller lambda foot with the shear layer of the larger separation zone [12].

For studying nozzles and their characteristics, experimental analysis is not practically sufficient as flow pattern and internal variables that cannot be measured easily by experimental work. Also, it is very difficult and an expensive affair to get the exact location of the shock along the nozzle length by experimental analysis. Therefore, numerical approach present work was adopted to focus on the study of different design and off design characteristics of bell type rocket nozzles. Less value of the mass flow rate in non-dimensional mass flow rate was considered to reduce the shape of the nozzle and save computational time. A code is developed in language C on the basis of the design that is obtained using the MOC and stream function. Using these data, the geometry of the bell nozzle is created in GAMBIT, and numerical simulation is carried out in FLUENT software with cold flow (Fluid: Air at 300K) and hot flow (Fluid: Hydrogen at 1000K) conditions. The numerical results are discussed in terms of such as pressure, temperature, velocity and Mach number. The presence of the different type of shock waves inside the nozzle are studied under the off design condition of over-expansion. A detailed comparison of numerical and analytical results is also done at the end.

2. Design of Bell Nozzle

A nozzle is designed to accelerate the flow to result in uniform, parallel and wave-free supersonic flow. The primary function of exhaust nozzles is efficient conversion of potential energy of the exhausting gas to kinetic energy by increasing the exhaust velocity, which is accomplished through efficiently expanding the exhausting gases to the ambient pressure. An improper contour will result in the presence of weak waves, which may coalesce to form a finite shock and prevent a uniform flow in the test section. The Method of Characteristics (MOC) is a numerical procedure appropriate for solving two-dimensional compressible flow problems [13]. The ideal nozzle designed with MOC is able to achieved uniform exit flow conditions [3]. The bell-shaped or contour nozzle had a high angle expansion section (20 to 50°) right behind the nozzle throat; this was followed by a gradual reversal of the nozzle contour slope so that the divergence angle was smaller at the nozzle exit (usually less than a 10° half angle) [2].

To carry out numerical simulation of a bell type nozzle, a computer code is developed in the C program. The code uses MOC and the stream function to define the higher efficiency nozzle contours for isentropic, inviscid, irrotational supersonic flows of any working fluid for any user-defined exit Mach number. The program starts with reading data from the user, such as enter the values of exit Mach number, throat radius, the number of divisions required at the initial expansion curve and the value of specific heat (γ). In the next step, the program evaluates the angle of divergence for the initial expansion contour downstream of the throat based on the exit Mach number that the user entered. After evaluating the values of θ , x , y , v , M , and μ for the points chosen on the initial curvature; using these values, the program evaluate all the properties on the intersection points of the characteristic lines based on theoretical formulas. At last, one can get the x , y coordinates of the divergent section of the nozzle based on obtained properties θ , v and M . The present design is carried out for an exit Mach number 3 and throat diameter 2 mm. The details of design parameters, obtained from the program, for cold flow (Fluid: Air at 300K) and hot flow (Fluid: Hydrogen at 1000K) are tabulated in Table 1.

Table 1: Details of design parameters for the bell type nozzle.

Nozzle with cold flow (working fluid: Air at 300K, $\gamma = 1.4$)			
Inlet Diameter, mm	4.0	Divergent length, mm	17.217
Exit Diameter, mm	8.446	Nozzle length, mm	21.217
Convergent length, mm	4.0		
Nozzle with hot flow (working fluid: Hydrogen at 1000K, $\gamma = 1.41$)			
Inlet Diameter, mm	4.0	Divergent length, mm	16.949
Exit Diameter, mm	8.304	Nozzle length, mm	20.949
Convergent length, mm	4.0		

3. Numerical Simulation

To understand the rocket nozzle performance under different flow conditions the numerical simulation is carried out in the CFD software GAMBIT 2.4.6 and FLUENT 6.3.26. The computational domain was modeled and meshed in GAMBIT as per design parameters represented in Table 1. Bottom-up approach is applied to create the fluid domain of nozzle geometry. Model geometry is meshed with structured grid consists of 25800 mesh faces. To have a good quality mesh it was required to split the computational domain in to the number of parts (faces), which allows a better mesh with low skewness. The nozzle geometry is divided into the number of zones and boundary conditions are applied. The inlet condition is given as the pressure inlet and the nozzle outlet is given as pressure outlet. Nozzle throat is given as an interior and nozzle surfaces are given as the wall. Figure 1 shows the meshed nozzle geometries with boundary conditions.

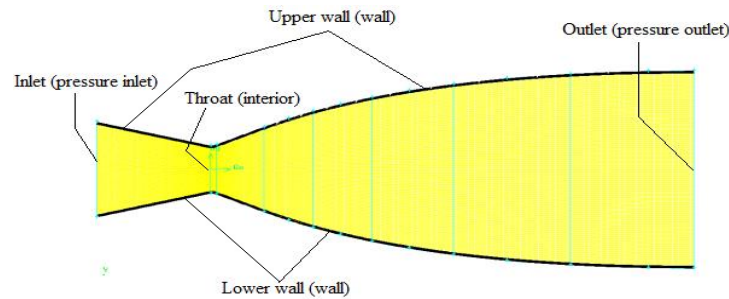


Fig. 1: The fluid domain with boundary conditions of the bell nozzle.

Meshed file, created in the GAMBIT 2.4.6 modeler, is imported in commercial CFD package FLUENT 6.3.26 and the FVM approach was adopted for flow simulation. The code Fluent has been used to solve 2-D steady state Reynolds-averaged Navier-Stokes (RANS) equations, with density based solver, in the nozzles for different flow conditions. Simulation is carried out with the zero operating pressure and Titanium as wall material. The choice of turbulence model had a significant influence on the simulated flow field in an over-expanded rocket nozzle. As per literature, the two equation model gave the best overall agreement with experimental pressure distribution at over expanded condition [14]. It was found that without corrections, standard two-equation turbulence model fails to predict the measured separation characteristics in the nozzle and results can be improved when a physical limiter of turbulent energy was introduced [15]. The Shear Stress Transport $k-\omega$ (SST $k-\omega$) model is used to simulate the flow through the nozzles. In this model the turbulent viscosity is modified to account for the transport of the principal turbulent shear stress. It is this feature that gives this model advantage in terms of performance over both the standard $k-\epsilon$ model and the standard $k-\omega$ model. In addition to this, a cross diffusion term in the equation and blending function to ensure that the model equations behave approximately in both the near-wall and far-field zones. From accuracy and convergence consideration, the second order upwind scheme was used for all the conservation equations after getting a convergence with the first order upwind scheme. Grid adaption based on the pressure gradient criterion was also invoked in order to capture the flow discontinuities accurately. With grid adaption, final solutions in most of the cases were obtained on grids that had 2 to 3 times the original number of cells. The convergence criteria for the residuals were set to $\epsilon^{(-4)}$. Once the solution gets converged, the contours of pressure, temperature, velocity and the Mach number are plotted.

4. Results and Discussion

Numerical analysis of the 2D bell nozzle is carried out at design pressure and off-design conditions for cold as well as hot flow conditions. The term design pressure condition indicates that the nozzle is operating at its design exit pressure, which gives a shock free isentropic flow. For cold flow analysis the flow is isentropically expands to a design pressure of 1atm with a stagnation temperature of 300K. Whereas; in the hot flow analysis, the Hydrogen gas at 1000K is expanded to 1atm pressure. Off-design condition is considering, the flow through the nozzle at the over-expanded condition with a shock wave inside the diverging section of the nozzle. In the off design analysis, the nozzle is operating at four different value of back pressure, i.e. 5 bar, 7 bar, 11 bar and 15 bar (for both cold and hot flow). Based on numerical simulations at design and off-design conditions, results are plotted in terms of variations in fluid properties like pressure, temperature, velocity and Mach number throughout the nozzle length. The results of simulation are compared with the analytical calculation based on 1D theory of compressible flow.

Table 2: The flow properties of the Bell nozzle at the different section for cold flow.

Properties	Nozzle Inlet		Nozzle Throat		Nozzle Outlet	
	Analytical	Numerical	Analytical	Numerical	Analytical	Numerical
Static Pressure, bar	34.881	34.93	19.662	22.298	1.013	1.025
Stagnation Pressure, bar	37.219	37.219	37.219	37.129	37.219	35.545
Static Temperature, K	294.49	294.6	250	259.2	107.14	111.07
Velocity, m/s	105.22	103.19	316.94	285.87	622.45	615.18
Mach number, M	0.306	0.3	1.0	0.886	3.0	2.932

Table 3: The flow properties of the Bell nozzle at the different section for hot flow.

Properties	Nozzle Inlet		Nozzle Throat		Nozzle Outlet	
	Analytical	Numerical	Analytical	Numerical	Analytical	Numerical
Static Pressure, bar	34.593	34.635	19.445	21.643	1.013	1.047
Stagnation Pressure, bar	36.925	36.925	36.925	36.809	36.925	34.908
Static Temperature, K	981.214	981.66	829.87	856.68	351.5	372.3
Velocity, m/s	732.98	717.836	2205.78	2014.85	4306.62	4215.31
Mach number, M	0.305	0.3	1.0	0.905	3.0	2.897

At first, the numerical and analytical analysis of the bell nozzle is carried out at design conditions for cold and hot flow. Details of flow properties, at different locations of nozzle, are represented in Table 2 and Table 3. Results reveals that the flow is continuously accelerating throughout the nozzle, therefore the pressure gets reduced from an inlet to an outlet of the nozzle. In both cold and hot flow analysis, a good agreement is observed between analytical and numerical results. In case of cold flow, the air with inlet velocity of 105.22 m/s get accelerated throughout the bell nozzle. At throat flow achieved velocity of 285.87 m/s whilst the sonic velocity is achieved after 0.5 mm distance from throat location. To get more idea about the Mach number near throat region; Mach number variations are plotted in the form of contours and graph as shown in Fig. 2. One can observe semicircular contour near the throat region and also the property variations after mid of diverging section is very less; which is a design characteristic of the bell nozzle. A little bit variation observed in Mach number values as in case of cold flow, at the exit of the nozzle a Mach number of 2.932 is obtained, which is 2.267 % lesser than the design Mach number. Whereas, the Mach number at the exit is 2.897 (3.43 % lower than the design Mach number) with a flow velocity of 4215.31 m/s (2.12 % lower than Analytical result) in case of hot flow analysis. The simulation results shows a Mach number of 0.905 (nearly the sonic Mach number) in case of hot flow. The small variations between numerical and analytical results are due to the assumption of constant stagnation pressure in the analytical case. Whereas; in the case of simulation, stagnation pressure loss occurs because of the boundary layer effects near the wall region. Thus, 4.49% and 5.46 % of total stagnation pressure loss is observed in simulation of cold and hot flow respectively.

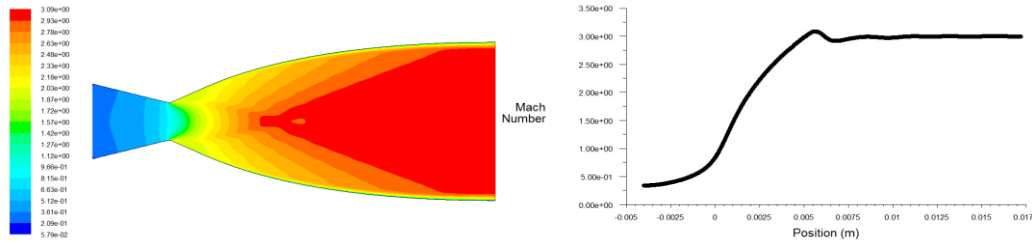


Fig. 2: Variations in Mach number along the axis of Bell nozzle for cold flow.

After satisfactory results of numerical analysis, the same nozzle is simulated for different off-design conditions for cold and hot flow. The off design performance of the bell nozzle is also analyzed in both analytical and numerical way. To carry out off design analysis, four different value of back pressure, i.e. 5 bar, 7 bar, 11 bar and 15 bar (for both cold and hot flow), are selected. The results of converged fluid domains, of cold and hot flow, are discussed here in details and compared with analytical one. To find the analytical location of shock, the calculations are carried out using shock theory with the assumption of steady one dimensional flow without body forces.

The results obtained from analytical analysis reveal that due to the off- design, back pressure effect, shock phenomenon occurs in the supersonic regions of the bell nozzle for back pressure value lower than the critical pressure. As the back pressure is reduced from 15 bar to 5 bar the shock developed is moving towards the exit of the nozzle. For the back pressure of 7 bar and 5 bar, the shock wave is captured outside of the nozzle for both cold and hot flow. However, the location of shock is different in both the cases of flow. It is also clear that, the strength of the shock is also going to increases when the back pressure is reduced. The shock corresponding to the back pressure of 15bar reduces the flow Mach number from 2.66 to 0.498 and for the back pressure of 5 bar, the shock decelerate the flow from Mach number 3.42 to 0.454 for cold flow. Whereas; these values are 2.665 to 0.5 and 3.376 to 0.4585 for 15 bar and 5 bar respectively in the case of hot flow. The stagnation pressure loss is increases as exit pressure reduces.

To get a clear idea about the flow behavior inside the bell nozzle, simulation of fluid domain is carried out at different off design back pressure. The results for the same are represented in the form of Mach number contours as shown in Fig. 3 and Fig. 4 for cold and hot flow respectively. It is clear from Fig. 3 and Fig. 4, that change in exit pressure from the design pressure create an over expanded flow through the nozzle. As a result, there is a presence of different types of shock wave phenomenon observed in the diverging area of the nozzle. Flow separation phenomena in a rocket nozzle is an unstable process caused by the downstream counter-pressure. The process of separation results from disturbances of the boundary layer, along the nozzle wall, that is unable to withstand an adverse pressure gradient, and finally separates. The separation location depends also on the turbulence in the boundary layer. Numerical analysis of the flow through the bell nozzle with a back pressure value of 15 bar (NPR=2.481), creates a shock pattern (Refer: Fig. 3-a and Fig. 4-a). In this flow regimes, the influence of shock wave boundary layer interaction starts from the throat itself. The contour shows both fully separated region and restricted separation region nearer to the upper and the lower wall respectively. There is a separation of flow occurs from the throat section such that, the flow nearer to the lower wall reattach after the separation whereas; in the upper wall the flow remains detached after the separation point. The shock wave after the throat, which is generated due to the abrupt pressure difference between the inner flow field and the ambient. These shock waves intersect and then interact with the shearing layer. As a result, a shock train is formed by expansion waves and compression waves that are similar to the free jet. Yang Yu et al was observed the similar shock train in the Schlieren image of the shock train [16]. In case of cold flow for the same back pressure, the shock train located near the lower wall of the diverging section. Literatures suggest the different position of the shock train for the different fluid as well as for the different configuration of the bell nozzle. But, till now nobody is able to justify the reason behind it. The variation of static pressure along the axis, upper and lower the wall of the nozzles are represented in the Fig. 5, where the green line represents the restricted shock separation at the upper wall and the red line indicate the free shock separation at the lower the wall after the throat section. After the throat section the flow separation started in both upper and lower wall, due to unsteadiness in the flow, the separated flow at the lower wall gets reattach to the wall. This reattachment of flow slightly increases the local static pressure after the reattachment point. In the upper wall, the flow remains detached, due to which the pressure line remains parallel to the x-axis after the throat section.

As the exit pressure reduced to 11 bar, the shock pattern is changed as shown in (Refer: Fig.3-b and Fig.4-b). At 11 bar exit pressure, a symmetric lambda shock inside the nozzle is observed instead of the shock train in case of the back

pressure 15 bar. The flow separation is symmetric and free shock separation occurs due to the detached flow near the upper and lower walls. The cap shock pattern is observed in which the triple point of the shock lies before the position of the reflection of the internal shock at the symmetric axis. A Mach stem is developed at a supersonic Mach number around 2.7 at the divergent nozzle section. A supersonic jet after the lambda shock as well as the reversible flow region is also observed clearly in figures. From Figure 6, it is clear that shock pattern corresponding to this exit pressure creates a symmetric shock train, which is formed by the combination of expansion and compression waves. It is also clear that both the upper and the lower wall shows similar pressure distribution throughout the nozzle. Figure 6-a shows a continuous expansion of flow up to the area at which shock is captured (5.4 mm diameter), after which flow compressed to 12.5 bar pressure at the centre line of nozzle. The flow separation starts 2.046 mm after the throat section, once the flow is detached the, pressure remains constant after the separation point, known as free shock separation and the flow remains detached. Whereas; the flow passes through the initial shock and the pressure rises from 2 bar to 25 bar in case of hot flow (Refer: Fig. 6-b). The flow again expanded through the expansion waves, this expanded flow enters into the next set of compression waves and diffusion takes place, this will repeat up to the exit of the nozzle. The compression waves only have approximately the half strength of the upstream shock. The pressure distribution exhibits, sharp oscillations which indicates that the flow decelerates through a normal shock, re-expands to higher speed, and again decelerate through the shock wave, re-expands, and so on, giving rise to aftershocks. Re-expansion may lead to local subsonic or supersonic velocities depending upon back pressure values. The after-shocks become stronger with the decrease in back pressure value.

In the case of 7 bar back pressure (Refer: Fig. 3-c and Fig. 4-c), the nozzle behaves exactly similar to the flow behaviour in the case of 11 bar, the only difference is that the location and strength of the shock are different. The Mach number contour (Refer: Fig.3-c) clearly shows the location of the Mach disc at a distance 8.1 mm from the throat section where the nozzle diameter is 7.14 mm. Due to the interaction of the shock wave (lambda foot) with the boundary layer, flow separation occurs in both upper and lower wall and separation is known as full shock separation. After the shock there is a local supersonic region is developed, flow downstream of the Mach disc is at subsonic condition. There is no reattachment of flow is observed once the flow gets detached, in both upper and lower wall the full shock separation is observed. The simulation data from Aeronautical Research institute [3] shows exactly similar flow pattern with present simulation results for the value of the 11bar and 7 bar back pressure. The lower and upper wall shows a similar pressure distribution throughout the nozzle length, after flow separation, the pressure remains unaffected near the nozzle wall as shown in Fig. 7. An adverse pressure gradient causes the boundary layer to detach from the nozzle wall surface. Due to strong shock wave boundary layer interaction, the nozzle experiences strong unsteadiness initiating the flow to detach from the boundary layer.

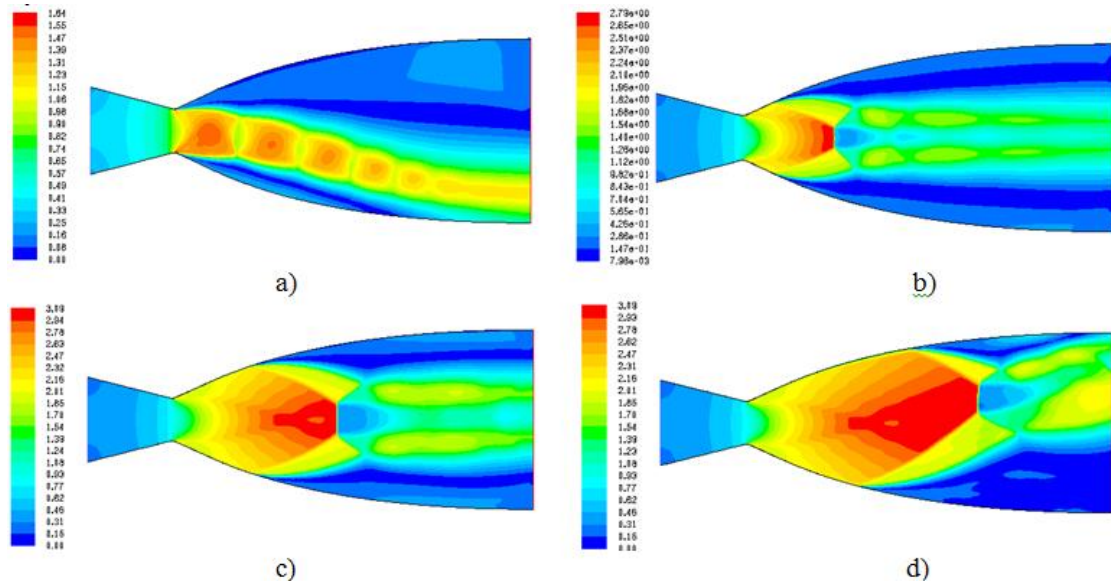


Fig. 3: Contours of the Mach number at different off-design back pressure for cold flow.
a) 15 bar b) 11 bar c) 7 bar d) 5 bar

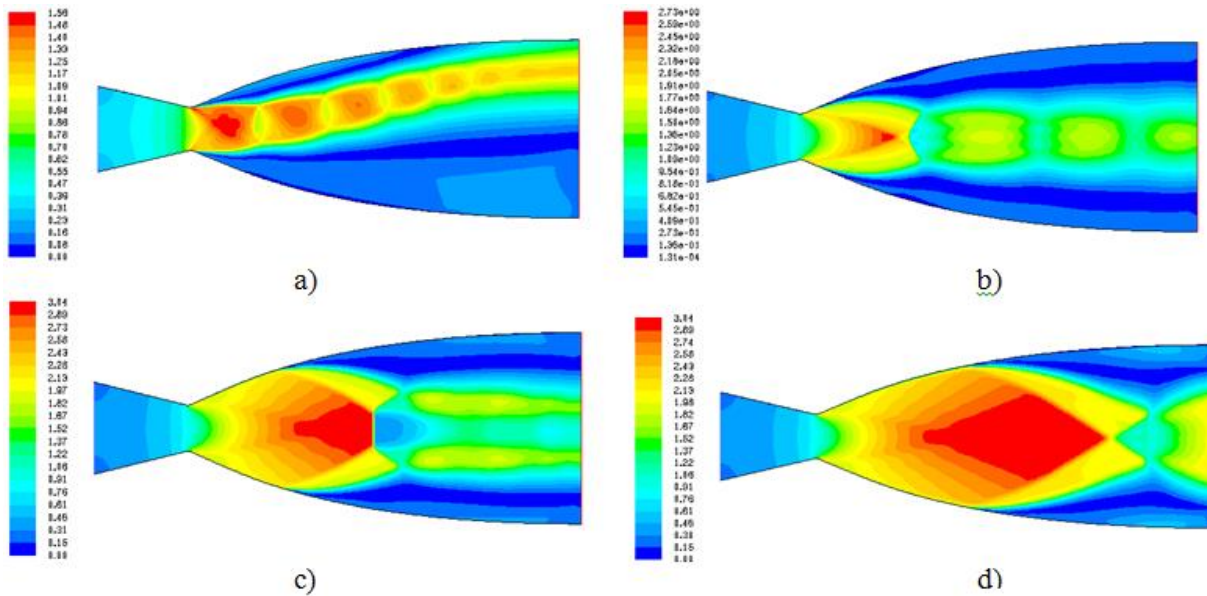


Fig. 4: Contours of the Mach number at different off-design back pressure for hot flow.
a) 15 bar b) 11 bar c) 7 bar d) 5 bar

The flow through the nozzle at 5 bar off-design condition captured asymmetric and symmetric lambda shock in case of cold flow and hot flow respectively (Refer: Fig. 3-d and Fig. 4-d). The flow pattern and properties are similar up to the throat section as in the case of design flow condition, the only flow changes occurred at the diverging section. Figures illustrate typical separated flow-field in an over expanded bell nozzle at a back pressure value of 5 bar. The shock in these cases take on a bifurcated structure consisting of an incident shock and a reflected shock merging into a Mach stem. The shock pattern is of Mach disc type, where the position of the internal shock lies ahead of the position of the normal shock at the symmetric axis. This is commonly referred to as a lambda foot, and the point at which the three components meet is called the triple point. The Mach stem is essentially a normal shock producing subsonic outflow. For the range of conditions of interest here, the incident and reflected shocks are of the weak type resulting in supersonic outflow past both. The adverse pressure gradient of the incident shock causes the boundary layer to separate and detach from the wall as shear layer that bounds the separation recirculation region. Figure 8 shows the comparison of enlarged view of the lambda shock obtained from the present simulation and the schematic representation of shock wave boundary layer interaction from literature [12]. The simulation result shows a good agreement with the actual flow.

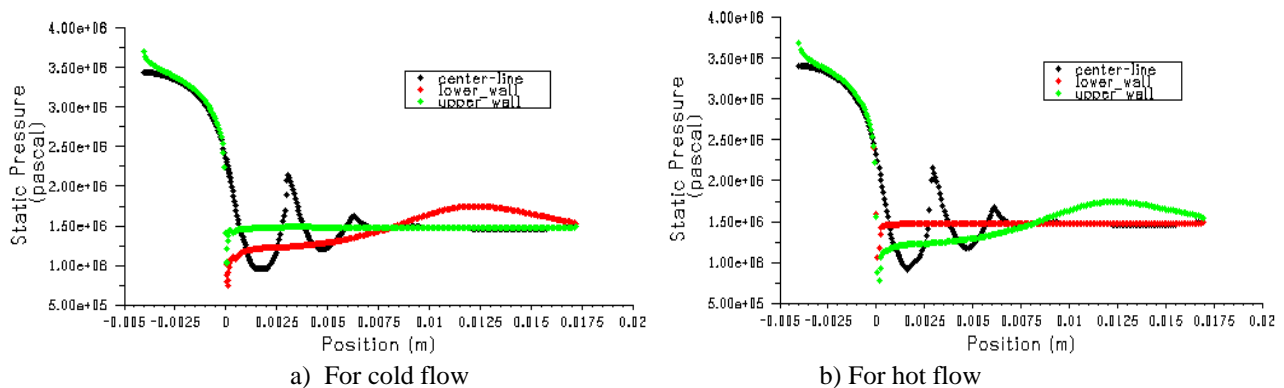


Fig. 5: Variation of static pressure along the axis and walls of the bell nozzle at 15 bar.

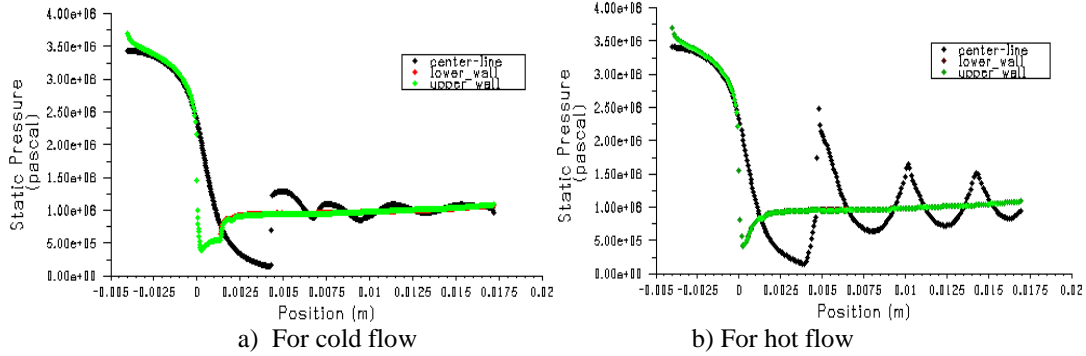


Fig. 6: Variation of static pressure along the axis and walls of the bell nozzle at 11 bar.

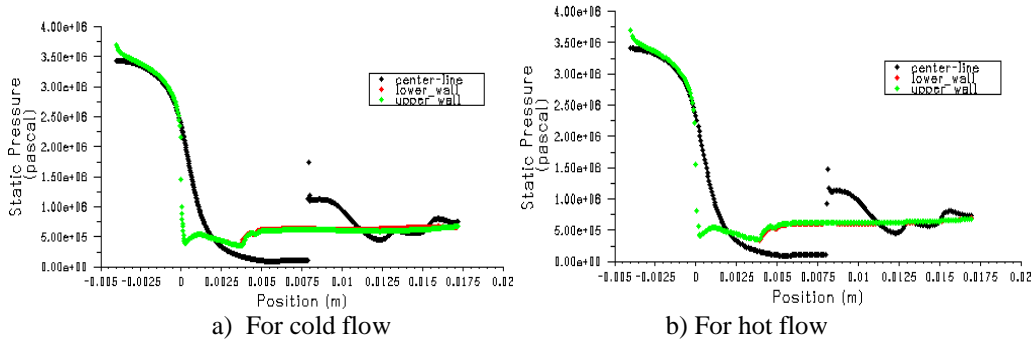
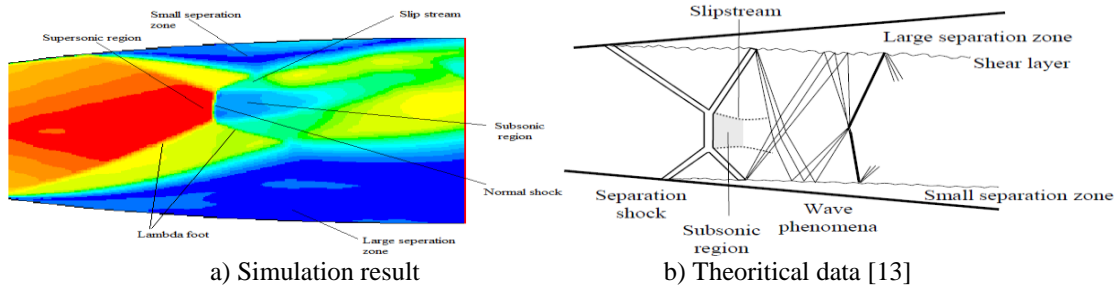
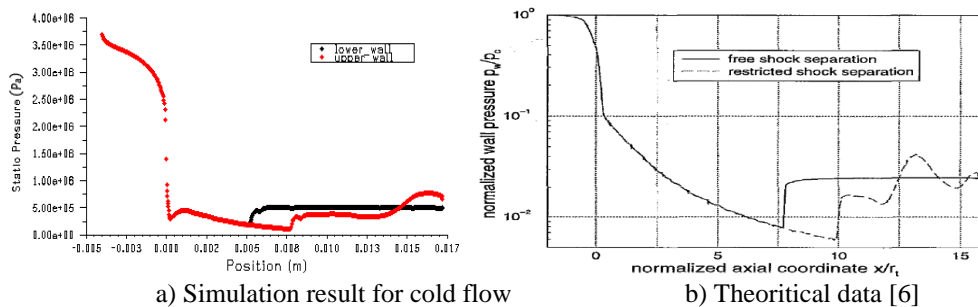


Fig. 7: Variation of static pressure along the axis and walls of the bell nozzle at 7 bar.



a) Simulation result
b) Theoretical data [13]
Fig. 8: Comparison of the lambda shock with the theoretical data.

The asymmetric pressure distribution near the upper and the lower wall, in case of cold flow, is due to the presence of asymmetric lambda shock (Refer: Fig. 9-a). The upper wall shows the Restricted shock separation (RSS) and in the lower wall, the Free shock separation (FSS) is developed. The wall pressure distribution in Fig. 9-a shows a similar nature as the pressure distribution explained by the Vulcaine engine [5]. The black line represents the free shock separation in the lower wall and the red line indicate the restricted shock separation near the upper wall.



a) Simulation result for cold flow
b) Theoretical data [6]
Fig. 9: Variations of Static Pressure along the lower and the upper wall.

Table 4: Details of the shock wave location for flow analysis of the bell nozzle.

Exit pressure (bar)	Cold flow (300 K)		Hot flow (1000 K)	
	Analytical result Diameter (mm)	Numerical result Diameter (mm)	Analytical result Diameter (mm)	Numerical result Diameter (mm)
15	3.66	2.48 (32%)	3.64	3.45 (5%)
11	4.34	5.40 (19%)	4.32	5.44 (20%)
7	5.51	7.14(23%)	5.47	7.06 (22%)
5	6.25	7.98 (18%)	6.47	7.96 (18.7%)

Finally, locations of the shock wave are calculated from simulation results for different back pressure in case of cold and hot flow analysis and compared with the analytical study. The location of the shock is defined in terms of the diameter of the diverging section. The details for the same are represented in Table 4. In analytical study all the equations used are defined for 1D flow whereas; in numerical analysis 2D flow is considered. Therefore, the location of lambda shock is very different in numerical results compared to that predicted by one dimensional inviscid theory. There is around 20% deviation observed in numerical and analytical results except the back pressure value 15 bar. For 15 bar pressure, the flow effect is more as deviation is 32% in case of cold flow whereas; 5 % in case of hot flow. For the value of 15 bar exit pressure, the usual normal shock does not sit alone, but is followed by aftershocks, which cannot be predicted by one dimensional inviscid theory. The simple inviscid theory obtains a normal shock followed by a smooth recovery to exit pressure, which differs from the results of numerical analysis. It is also observed that the change of fluid affects the location of the shock as well as the behaviour of shock pattern.

5. Conclusions

The 2D axi-symmetric flow analysis is carried out within the bell type nozzle, at design and off-design conditions, by using computational fluid dynamic software GAMBIT 2.4.6 and FLUENT 6.3.26. Simulation has been carried out separately for two different flow conditions i.e. cold and hot. The following conclusions are made from analysis:

- 1.The converged solutions captured the asymmetric lambda shock in the nozzles at higher nozzle pressure ratios (NPR) for viscous flows. It also predicted aftershock and flow separation depending upon NPR.
- 2.The strength of normal shock, at Mach stem in viscous prediction, generally increases with an increase in NPR.
- 3.Good agreement is observed between predicted simulation and analytical results in terms of shock structure, shock location, the size of normal shock, aftershock, and asymmetric lambda shocks. However, there is a significant variation in location of shock, as the shocks predicted sits at a different diameter than that estimated from analytical study.

References

- [1] G. Hagemann, H. Immich and T. Van Nguyen, "Advanced Rocket Nozzles," *Journal of Propulsion and Power*, vol. 14, no. 5, 1998.
- [2] G. P. Sutton, *Rocket Propulsion Elements*, 7th ed, 2001.
- [3] J. Ostlund, "Flow Process in Rocket Engine Nozzles with Focus on Flow Separation and Side-Loads," *Licentiate Thesis, Stockholm*, 2002.
- [4] J. Mattsson, U. Hogman, L. Tornngren, "A Subscale Test Programme on Investigation of flow Separation and Side Loads in Rocket Nozzles," *Proceedings of the Third European Symposium on Aerothermodynamics for Space Vehicles*, 1998.
- [5] M. Frey and G. Hagemann, "Flow Separation and Side-Loads in Rocket Nozzles," *Joint Propulsion Conference & Exhibit*, 1999.
- [6] A. Grob and C. Weiland, "Investigation of Shock patterns and Separation behavior of Several Subscale Nozzle," in *36th AIAA/ASME/SAE/ASEE Joint Propulsion Conference & Exhibit*, 2000.
- [7] G. Hagemann, M. Frey and W. Koschel, "Appearance of Restricted Shock Separation in Rocket Nozzles," *Journal of Propulsion and Power*, vol. 18, no. 3, 2002.

- [8] S. Bhushan Verma, R. Stark, O. Haidn, "Relation between shock unsteadiness and the origin of side-loads inside," *Aerospace Science and Technology*, Elsevier, 2006.
- [9] J. H. Ruf, D M. McDaniels, A M. Brown, "Details of Side Load Test Data and Analysis for a Truncated," *American Institute of Aeronautics and Astronautics*, 2009.
- [10] R. H. Stark and B. H. Wagner, "Experimental Flow Investigation of a Truncated Ideal Contour Nozzle," *37th AIAA Fluid Dynamics Conference and Exhibit*, 2010.
- [11] P. Reijasse, B. Corbel, D. Soulevant, "Unsteadiness and Asymmetry of Shock-Induced Separation in a Planar Two-Dimensional Nozzle: A Flow Description," *30th AIAA Fluid Dynamics Conference*, Norfolk, VA, 1999.
- [12] D. Papamoschou and A. Johnson, "Unsteady Phenomena in Supersonic Nozzle Flow Separation," *36th AIAA Fluid Dynamics Conference and Exhibit*, San Francisco, California, 2006.
- [13] J. D. Anderson Jr., *Computational Fluid Dynamics the Basics with Applications*. McGraw-Hill Company (Original version), 2002.
- [14] P. Natta, V. Ranjith Kumar and Y. V. Hanumantha Rao, "Flow Analysis of Rocket Nozzle Using Computational Fluid Dynamics," *International Journal of Engineering Research and Applications (IJERA)*, vol. 2, no. 5, 2012.
- [15] J. Ostlund and M. Jaran, "Assessment of turbulence models in over expanded Rocket nozzle Flow Simulations," *Presented at 35th AIAA/ASME/SAE/ASEE Joint Propulsion Conference and Exhibit*, AIAA Paper 99-2583, 1999.
- [16] Y. Yu, J. Xu, J. Mo and M. Wang, "Principal Parameters in Flow separation Patterns of Over-expanded Single Expansion Ramp Nozzle," *Engineering Applications of Computational Fluid Dynamics*, vol. 8, no. 2, 2014.